IJNRD.ORG ISSN : 2456-4184
INTERNATIONAL JOURNAL OF NOVEL RESEARCH AND DEVELOPMENT (IJNRD) | IJNRD.ORG
An International Open Access, Peer-reviewed, Refereed Journal

STUDY OF INTEGRATED CMOS TRANSMIT-RECEIVE SWITCH AND FORMULATION OF HIGH FREQUENCY SPIRAL INDUCTOR MODEL

JAWED AKHTER[1], DR. K. B. SINGH[2], PROF. SURENDRA ROY[2]
[1]University Deptt. of Physics, B. R. A. Bihar University, Muzaffarpur, Bihar, India-842001.
[2]Deptt. of Physics, L. S. College, Muzaffarpur, Bihar, India-842001.

ABSTRACT
In this paper, we report on study of formulation of high frequency spiral inductor model. The spiral inductor is a critical component of this technique and a new compact model is proposed and verified by simulation and experiment. The spiral inductor model is incorporated in a tool which allows quick synthesis and analysis of spiral inductors across a variety of geometries and substrate doping. The enormous potential of the wireless communications market, the low level of integration of current transceiver implementations, and the rapid advance of low-cost silicon processing technologies, have contributed to the renewed interest in radiofrequency (RF) circuit design in the last decade. Although Metal-Oxide-Semiconductor-Field-Effect-Transistor (MOSFET) characteristics as a switch have dramatically improved over the years, its performance still falls short of the specifications needed in an RF transceiver [1].

Keywords: RF Switch, MOSFET, Spiral Inductor.

1. INTRODUCTION
The interest in low-cost, low-power, silicon-based transceiver designs for radio-frequency (RF) applications, such as cell phones and wireless networking, has prompted research in wireless circuit design techniques using complementary-metal-oxide-semiconductor (CMOS) technology. A critical limitation in obtaining fully integrated CMOS wireless systems is the lack of high-quality switches [2]. The spiral inductor is a critical component of this technique and a new compact model is proposed and verified by simulation and experiment. The spiral inductor model is incorporated in a tool which allows quick synthesis and analysis of spiral inductors across a variety of geometries and substrate doping. Using the optimized spiral inductors, a T/R switch is designed for 5-GHz applications in a 0.18-mm standard digital CMOS technology. Measurements of the prototype reveal that the switch does meet the targeted specifications.

2. EXPERIMENTAL VERIFICATION
Experimental verification of this model was carried out by fabricating several spiral inductor geometries on a variety of substrates in the Stanford Nanofabrication Facility.

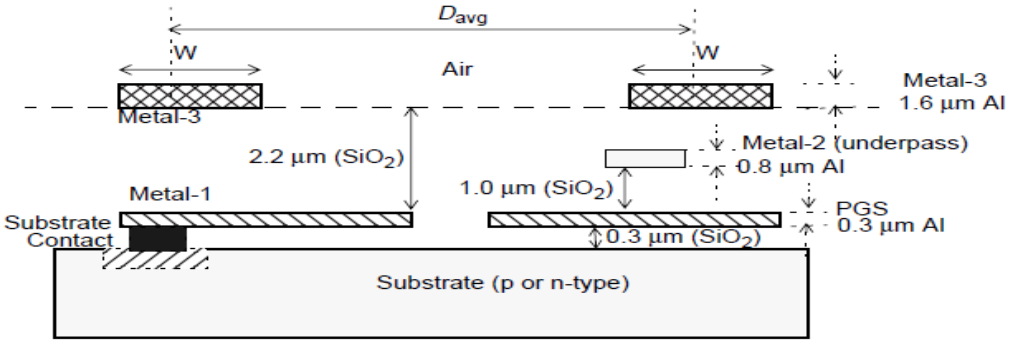

Figure 1: Spiral inductor cross-section showing the various layers. Metal-3 is used for creating the turns of the spiral with the underpass located in metal-2. The PGS is designed in metal-1.

Test Structure Fabrication:

A six-mask process using deposited silicon-dioxide, εr=4, as insulator and sputtered Aluminium, ρ = 2.9e7S/m, as metal was designed and developed for making test structures. The process cross-section is shown in Figure 3.35. The substrate is connected in all the cases and shorted, along with the PGS, to the ground pad. The PGS is of 'X' shape and made in metal-1 to ensure minimal loss in the substrate. Consequently, the remaining loss mechanisms dominate performance.

Five wafer splits, K2, I2, H2, M2, and L2, are used with substrate dopings of 13, 0.64, 0.084, 0.036, and 0.018 Ω-cm, respectively. The least doped substrate, ρ_{sub} = 13 Ω-cm, is typical of starting silicon in a bulk technology, while the highest doped substrate, ρsub = 0.018 Ω-cm, is typical for an epi technology. A set of geometries, shown in Table 1, with multiple outer diameters (D_{out}), widths (W), and number of turns (N), were fabricated for each of the five splits. The probe pads used for measuring the test structure introduce an unwanted parasitic capacitance in the measurements. All test structures are accompanied by structures to subtract out the effects of the pad capacitance.

Table 1: Spiral inductor test structure matrix.

Split	Substrate ρ (Ω-cm)	Inductor geometries		
		W (μm)	D_{out} (μm)	N
K2	13	5 – 10	100 – 300	1 – 8
I2	0.64	5 – 10	100 – 300	1 – 8
H2	0.084	5 – 10	100 – 300	1 – 8
M2	0.036	5 – 10	100 – 300	1 – 8
L2	0.018	5 – 10	100 – 300	1 – 8

3. MEASUREMENTS AND RESULTS

One-port S-parameter measurements were carried out using the HP8510 network analyzer. The standard technique of 'Short-Open-Load' calibration was used to ensure accurate measurements [3][4]. After subtracting the effects of the pad capacitance, the measured S-parameters are transformed to input impedance Z_{in}. Inductor Q is calculated as the ratio of the imaginary part of Z_{in} to the real part.

The effect of various substrate dopings is illustrated in Figure 2. The most heavily doped sample shows a peak quality factor reduction of almost 35% as compared to the most lightly doped sample for the given geometry. The rapid rise of resistance with frequency is the main cause of the lower peak-Q frequency in heavily doped samples. The model uses α = 3.3, which is the same value used in the modeling of transmission lines. The measurements also confirm the model prediction that bulk technologies, ρ_{sub} ~ 13 Ω-cm, do not suffer from magnetic field induced losses in the substrate.

For a given inductor, the effect of substrate doping decreases for lower frequencies. Lower frequency, f ~ 1 GHz, RF circuits, however, often require larger inductances, which correspond to a larger D_{out} and an increased number of turns. Therefore, eddy current induced substrate loss cannot be neglected at lower frequencies as it increases rapidly with both these factors. Measured results in Figure 3.37 show that, even at 1.2 GHz, a 10 nH inductor suffers from Q-factor reduction as large as 25% in an epi-type wafer, L2, when compared to a bulk-like wafer, K2.

Figure 3 (a), (b) illustrate the model performance with respect to geometry for heavily as well as lightly doped substrates. Spiral inductors on lightly doped substrates suffer primarily from skin and proximity effect. The model predicts these phenomena well in Figure 3(a) for several geometries. For spiral geometries on heavily doped substrates, the eddy current losses are significant. Figure 3(b) confirms the accuracy of the eddy current substrate loss model for a variety of geometries.

While the previous plots verify that Q is well modeled, the modeling of the real and imaginary parts of the measured impedance need to be separately verified. Figure 4(a) and (b) compare the effective resistance, Real(Z_{in}), and inductance, Imag(Z_{in})/ω, respectively, for a spiral inductor on heavily and lightly doped substrates. The effective resistance is much higher and the effective inductance is lower in the epi-type sample.

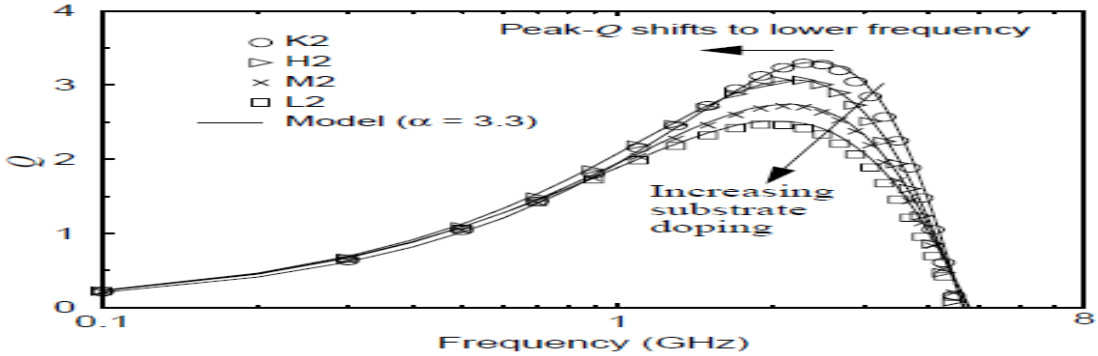

Figure 2a: Effects of increasing substrate conductivity on *Q*. Higher doping leads to decreased *Q*. *D*out = 250 μm, *W* = 5 μm, *N* = 4, *L*dc = 7.88 nH.

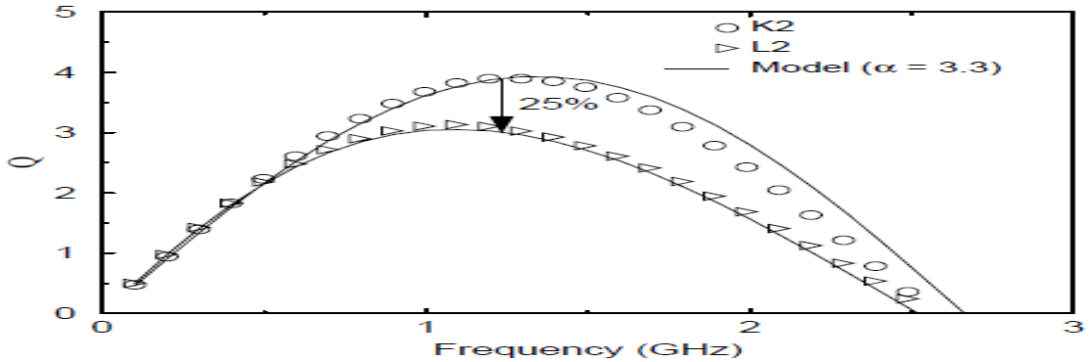

Figure 2b: Effect of substrate doping for a 10-nH inductor at lower frequencies. Even at 1.2 GHz, the heavily doped sample shows 25% degradation. D_{out} = 250 μm, *W* = 10 μm, *N* = 8.

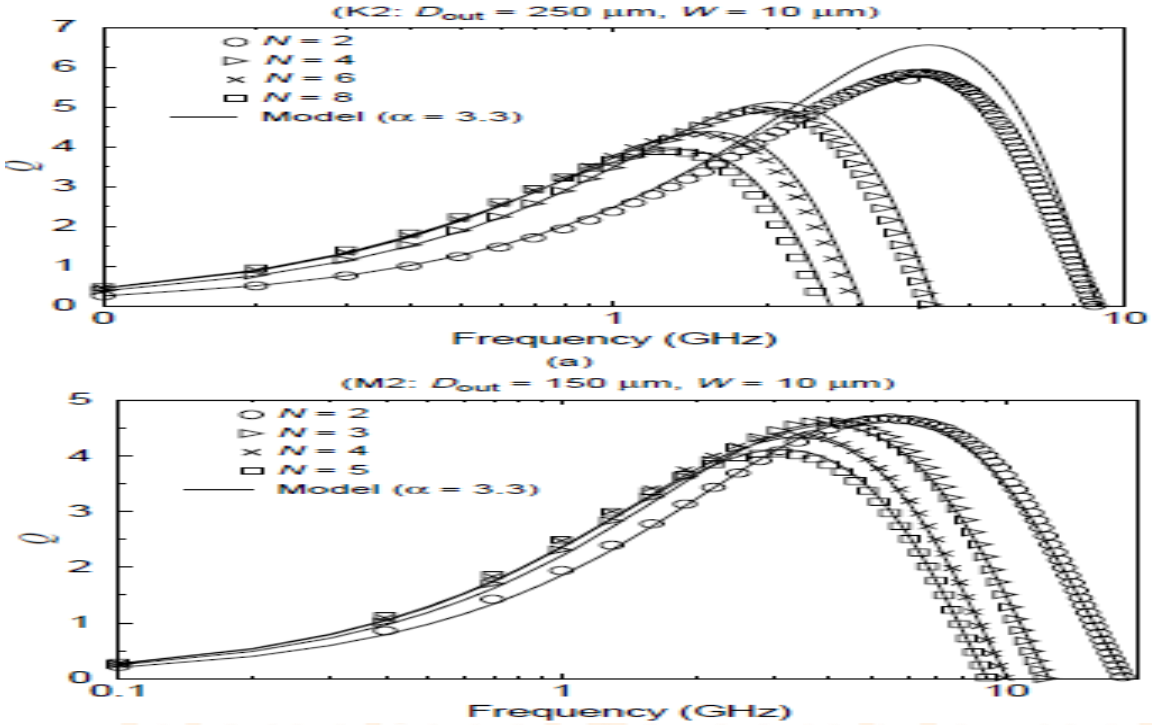

Figure 3: Model performance with respect to geometry for (a) Lightly doped sample, K2, and (b) Heavier doped sample, M2. Skin and proximity effect models can be evaluated in (a), while models for eddy current loss in the substrate can be evaluated in (b).

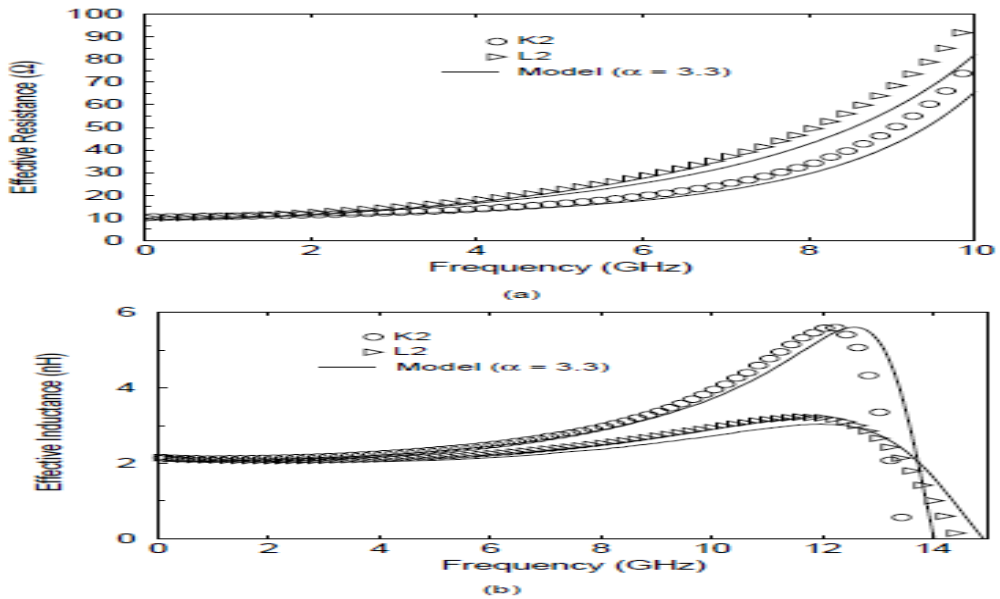

Figure 4: Effect of epi vs. non-epi substrate dopings on (a) Effective resistance, and (b) Effective inductance. D_{out} = 200 μm, *W* = 5 μm, *N* = 3.

The overall model performance is summed up in Figure 3.40. Model error across all different substrates and inductor geometries is mostly less than 10% including errors due to process variations and measurements. The model uses the value of $\alpha = 3.3$ for all the test structures.

4. CONCLUSIONS

RF circuit design requires accurate modeling and characterization of spiral inductors for a variety of technologies at high frequencies. This paper studies the principal phenomena affecting spiral inductor performance at RF, viz. shield parasitics, skin and proximity effects, and eddy current substrate loss. A new PGS design is developed and shown to be near optimal. A physics-based model is developed to provide qualitative and quantitative insight into the RF phenomena. The proposed model is verified using 2-D simulations and measurements. A web-based modeling tool is developed and described to assist RF circuit designers in quick analysis and synthesis of inductors.

REFERENCES

[1] P.R. Gray and R.G. Meyer, "Future directions in silicon ICs for RF personal communications," *Proceedings of the IEEE 1995 Custom Integrated Circuits Conference*, pp. 83-90, May 1995.
[2] L.E. Larson, "Integrated circuit technology options for RFICs - present status and future directions," *IEEE Journal of Solid-State Circuits*, Vol. 33, No. 3, pp. 387-399, March 1998.
[3] D. Su *et al.*, "A 5GHz CMOS transceiver for IEEE 802.11a wireless LAN," *ISSCC Digest of Technical Papers*, pp. 92-93, February 2002.
[4] G. Chien *et al.*, "A 2.4GHz CMOS transceiver and baseband processor chipset for 802.11b wireless LAN application," *ISSCC Digest of Technical Papers*, pp. 358-359, February 2003.
[5] W. Kluge *et al.*, "A 2.4GHz CMOS transceiver for 802.11b wireless LANs," *ISSCC Digest of Technical Papers*, pp. 360-361, February 2003.
[6] B. Razavi, *RF Microelectronics*, New Jersey: Prentice Hall PTR, 1998.
[7] F-J Huang, and Kenneth O, "A 0.5-mm CMOS T/R Switch for 900MHz Wireless Applications," *IEEE Journal of Solid-State Circuits*, Vol. 35, No. 3, pp. 486-492, March 2001.